

Ref No-3

FE Analysis and CAD of Radial-Flux Surface Mounted Permanent Magnet Brushless DC Motors

Parag R. Upadhyay^{1,2} and K. R. Rajagopal¹, *Senior Member, IEEE*

¹Department of Electrical Engineering, Indian Institute of Technology Delhi, New Delhi 110016, India

²Nirma University of Science and Technology, Ahmedabad 382481, India

DELNET

In this paper, a comprehensive computer-aided design (CAD) procedure for a radial-flux surface mounted permanent magnet brushless dc motor is presented. The design variables such as airgap flux density, slot electric loading, winding factor, stacking factor, stator current density, slot space factor, magnet fraction, slot fraction, flux density in the stator back iron, etc., are assumed. The basic output equations are derived and used for the design algorithm. The developed CAD program gives the design data and the calculated performances of the motor. Three different motors of rating 70 W, 2.2, and 20 kW are designed using the developed program and then finite-element analyses are carried out to validate the designs.

Index Terms—Brushless motor, computer-aided design (CAD) of motor, finite-element (FE) analysis, motor, permanent-magnet (PM) motor, permanent-magnet brushless dc (PM BLDC) motor.

I. INTRODUCTION

PERMANENT-MAGNET brushless dc (PM BLDC) motors are increasingly used in various domestic and industrial applications. Among the various types of PM BLDC motors, the radial-flux, surface mounted type is easy to fabricate. Performance equations for torque, inductance, etc., of the PM BLDC motor are available in literature [1], [2]. Development of a computer-aided design (CAD) program for the design and performance evaluation of radial-flux surface mounted PM BLDC motors is attempted and the details of the steps involved along with a flow chart and recommendations is given in this paper. The design data of the motor obtained from this program, if needed, can be used as the input for further optimization of the designs using finite-element (FE) techniques. The design algorithm includes a complete design procedure, data libraries like standard wire gauge, magnetic material properties, etc., and an interactive input and output facility. Three different motors of rating 70 W, 2.2 kW, and 20 kW are designed using the developed program. These motors were analyzed using two-dimensional (2-D) FE techniques and the validity of the developed CAD program is established.

II. OUTPUT EQUATIONS OF RADIAL-FLUX PM BLDC MOTOR

Based on the expressions for the torque and back EMF [1], [2], the output equation for the radial-flux PM BLDC motor, is derived as follows, where P_o is the rated power output, ω_m is the rated speed, L is the active motor length, D_{ro} is rotor outer diameter, T is motor developed torque, N_c is the number of coils conducting simultaneously, N_m is the number of poles, N_{spp} is the number of slots/pole/phase, K_w is the winding factor, B_g is specific magnetic loading, and I_s is specific slot loading

$$\begin{aligned} P_o &= T\omega_m = \eta N_c E_{ph} I_{ph} \\ T &= \frac{P_o}{\omega_m} = \frac{\eta N_c E_{ph} I_{ph}}{\omega_m} \end{aligned} \quad (1)$$

$$\begin{aligned} &= \frac{\eta N_c (N_m N_{spp} K_w B_g L D_{ro} n_s \omega_m / 2) I_{ph}}{\omega_m} \\ &= \frac{\eta N_c N_m N_{spp} K_w B_g L D_{ro} I_s}{2T} \\ \therefore LD_{ro} &= \frac{2T}{\eta N_c N_m N_{spp} K_w B_g I_s} \end{aligned} \quad (2)$$

Rather than taking the specific electric loading in PM BLDC motors, a specific slot loading I_s can be considered in the design with advantage [1]. The LD_{ro} product depends on the torque developed by the motor, specific magnetic loading, specific slot loading, and the efficiency, as shown in (2). The output equation can be modified as given below, and by selecting appropriate D_{ro}/L ratio, the rotor outer diameter and the length of the motor can be worked out

$$LD_{ro} = \frac{2}{(\eta N_c N_m N_{spp} K_w B_g I_s)} \left(\frac{P_o}{\omega_m} \right) \quad (3)$$

III. IMPORTANT DESIGN CONSIDERATIONS

A. Magnet Materials

Nd-Fe-B and samarium cobalt permanent magnets are preferred because of their high-energy product (BH_{max}) and retentivity (B_r). The selection depends on the cost and the operating temperature. The choice of soft magnetic material for stator and rotor core depends on frequency and operating flux density. As negligible flux reversal occurs at the rotor back iron, the choice can be on flux density alone. If volume is low and cost is not as important as performance, the use of M-19 of either 29-gauge or 26-gauge is recommended [1].

B. Winding, Stacking, and Slot Space Factors

Winding factor depends on the pitch factor, distribution factor, and the skew factor; this can easily be calculated. The stacking factor is considered based on the stamping grade; for 29-gauge lamination, the stacking factor recommended is 0.9 [1]. The slot space factor is taken based on the phase voltage and the current density.

C. Current Density

The current density between 4–10 A/mm² is generally recommended for PM motor windings [2], based on the cooling method employed. The lower range is advisable for small and totally enclosed motors. For high efficiency, still smaller current densities can be used, but with higher size and cost for the motor.

D. Specific Loadings

Specific magnetic loading depends on the type of configuration and permanent magnet properties. The use of rare earth magnets may allow the value of B_g to be as high as 0.9 T. Higher values of specific slot electric loading I_s leads to increase in copper loss; but because of the reduction in the permanent magnet requirement, reduces the overall cost. On the other hand, low value of I_s gives high efficiency, but necessitates huge quantity of permanent magnet material resulting in increased cost.

E. Number of Magnet Poles

For the fixed main dimensions, with the increase in the number of poles (N_m), either the width of magnet spacer or the magnet fraction will decrease, which will result in decrease in specific magnetic loading and thereby the developed torque also. End turn becomes shorter for higher N_m , which reduces the phase resistance, thereby increased efficiency. The leakage inductance for higher N_m is less, but with increase in the drive frequency.

F. Length of Airgap

Of the three components of the phase-inductance, the airgap inductance is the predominant. Larger airgap will result in reduced phase-inductance, armature reaction effects, and also the cogging torque, but will necessitate bigger magnets, thereby increased cost.

IV. CAD OF SURFACE-MOUNTED RADIAL-FLUX PM BLDC MOTORS

The flow chart of the developed CAD program for the surface-mounted radial-flux PM BLDC motor is given in Fig. 1. The airgap flux density, slot electric loading, winding factor, stacking factor, stator current density, slot space factor, magnet fraction, slot fraction, flux density in the stator back iron, etc., are assumed as fixed input parameters in the design. The phase current is decided by the power requirement and induced EMF decides the number of conductors per slot. The outer loop is to set and correct the assumed efficiency. The inner loop is for reducing the difference between the assumed and actual flux densities by changing the length of the magnet. Motor specifications, type of configuration, material types, and other assumed data for the design are provided as the input. As given in the flow chart of the developed CAD program in Fig. 1, the calculation of the main dimensions, stator design, permanent magnet rotor design, performance calculations, and the data sheet generation are the main five stages of the design procedure.

Three motors of ratings: 1) 24 V, 70 W, and 350 rpm; 2) 230 V, 2.2 kW, and 1450 rpm; and 3) 230 V, 20 kW, and 1500 rpm are

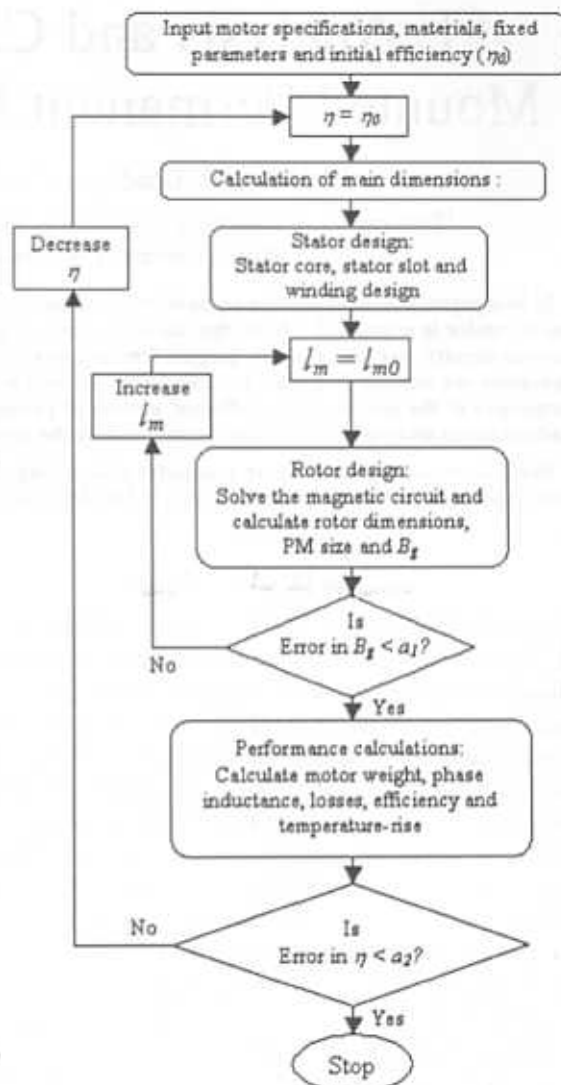


Fig. 1. Flowchart for CAD of PM BLDC motor.

designed using the developed CAD program. Important parameters and performance of the motors are given in Table I. It is observed that: 1) the efficiency increase with the rating; 2) the phase-inductance is more when the voltage is more; and 3) for the same voltage, the phase-inductance decreases with increase in the power rating.

The increase in magnet fraction will lead to substantial increase in iron volume and decrease in permanent magnet volume. From the parametric analysis of the 70 W motor using the developed CAD program, it is observed that the motor weight will initially decrease, and then increase with the increase in the magnet fraction or the slot fraction. No considerable changes observed in efficiency, copper weight, and temperature-rise of the motor with the increase in magnet fraction.

V. VALIDATION OF THE CAD RESULTS BY FE ANALYSIS

The accuracy of the developed CAD program is established by conducting 2-D FE analyses of the designed motors with two of the three phases excited at a time with rated current fed to the phase windings. Figs. 2–4 give the flux density plots of the 70

TABLE I
DESIGN OUTPUTS OF THE PM BLDC MOTORS OBTAINED
USING THE DEVELOPED CAD PROGRAM

Performance	70 W motor	2.2 kW motor	20 kW motor
Full load efficiency (%)	84.75	94.22	96.47
Stator outer diameter (mm)	92	169	325
Length of motor (mm)	45	104	217
Inductance per phase (mH)	4.9	7.1	0.9
Total weight of motor (kg)	2.39	13.86	101.28

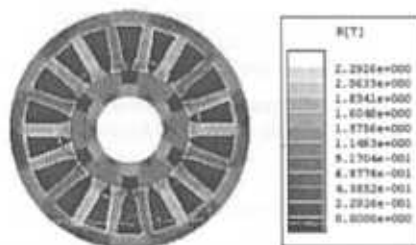


Fig. 2. Flux density plot of the 70 W PM BLDC motor.

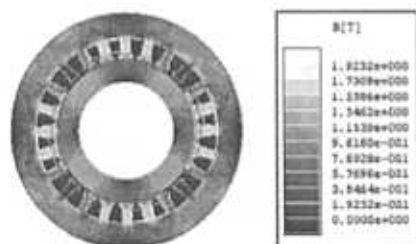


Fig. 3. Flux density plot of the 2.2 kW PM BLDC motor.

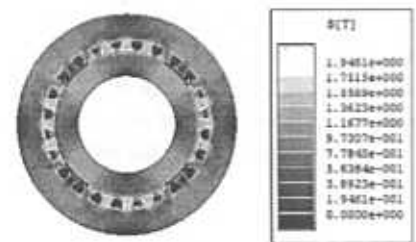


Fig. 4. Flux density plot of the 20 kW PM BLDC motor.

W, 2.2 kW, and 20 kW motors, respectively, obtained from the FE analyses; these figures also helps in visualizing the geometry of the motors.

The torque versus angle characteristics of the designed 70 W PM BLDC motor, obtained using FE analysis by giving constant currents in two phases of the motor in appropriate switching cycle, is given in Fig. 5. Similar torque characteristics are ob-

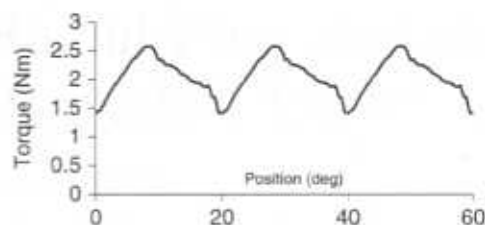


Fig. 5. Torque profile of the designed 70 W PM BLDC motor.

TABLE II
COMPARISON OF CAD AND FE ANALYSIS-BASED RESULTS OF
THE DESIGNED PM BLDC MOTORS

Developed Torque (Average)	70 W motor	2.2 kW motor	20 kW motor
Design target (Nm)	1.91	14.49	127.32
Computed by CAD (Nm)	1.91	14.60	135.93
Computed by FE analysis (Nm)	2.03	13.79	124.6
Error between the target and FE based values (%)	+6.28	-4.83	-2.13

tained for the other two motors also, and the average torques developed in all the motors are tabulated in Table II, which also gives the comparison between the CAD and FE analysis-based results. It is observed that the results are within the acceptance tolerance; however, the minor difference between the two can be attributed to the empirical design coefficients and formulae used in the CAD program.

VI. CONCLUSION

A comprehensive CAD procedure involving the derivation of the output equation and two self-corrective loops; one for the efficiency and the other for the airgap flux density for the surface-mounted radial-flux PM BLDC motor is discussed. Three designs, one each in fractional, low, and medium hp categories arrived at using the developed CAD program are giving the targeted torque within an acceptable tolerance band; but with high efficiencies. The CAD-based designs are validated using the FE analyses.

REFERENCES

- [1] D. C. Hanselman, *Brushless Permanent Magnet Motor Design*. New York: McGraw-Hill, 1994.
- [2] I. R. Handershot and T. J. E. Miller, *Design of Brushless Permanent Magnet Motors*. Oxford, U.K.: Oxford, 1994.
- [3] F. B. Chaaban, "Determination of the optimum rotor/stator diameter ratio of permanent magnet machines," *Elect. Mach. Power Syst.*, vol. 22, no. 4, pp. 1679-1685, Jul/Aug. 1980.

Manuscript received February 7, 2005.